How to Cite:
Dashti, A., Mohammad, F. A., & Ibrahim, M. J. (2022). Geochemistry study of black shale in Barzewa and Warte Sections, Sargelu Formation, Kurdistan Region, Iraq. *International Journal of Health Sciences*, *6*(S6), 8118–8134.
https://doi.org/10.53730/ijhs.v6nS6.12227

Geochemistry study of black shale in Barzewa and Warte Sections, Sargelu Formation, Kurdistan Region, Iraq

Dashti A.
Chemical and Petrochemical Department, Engineering Collage, Salaheddin University, Erbil/Iraq
*Corresponding author email: dashti.sulaiman@su.edu.krd

Dr. Farhad A. Mohammad
Department of Earth science and petroleum, Science Collage, Salaheddin University, Erbil/Iraq
Email: farhad.mohammad@su.edu.krd

Dr. Mohammed J. Ibrahim
Chemical and Petrochemical Department, Engineering Collage, Salaheddin University, Erbil/Iraq
Email: mohammed.barzanjy@su.edu.krd

***Abstract*---**Sargelu Formation (Middle Jurassic) is characterized by a wide geographical distribution in Iraq and neighboring countries. This study includes two sections Barzewa and Warte locations in Erbil Governorate of Kurdistan region, Iraq, the organic, inorganic Geochemistry and mineralogical properties were recorded. Fifteen samples of Sargelu Formation black shales were gathered from both locations. The source rocks of the black shales have an intermediate to felsic composition. The illite crystallinity index (IC) of the studied black shale shows the high anchizone stage. The organic geochemical parameters were analyzed in Sargelu Formation, the black shale contains type II - III kerogen. The average total organic carbon (TOC) of black shale for both section is 4.29 wt.%. By using the ultrasound homogenizer process the C-H bond (hydrocarbon component) of black shale recovered from the solid state to the liquid state.

***Keywords*---**geochemistry, mineralogy, black shale, ultrasound, FTIR spectrum.

Introduction

Sargelu Formation is one of the most well-known formations in the Middle Jurassic successions because of TOC contains up to 28% (Abdula et al., 2015, Al-Ameri and Al-Nagshbandi, 2015, Al-Ameri et al., 2014, Aqrawi et al., 2010, Buday, 1980, Jassim and Goff, 2006). The Two sections (Barzewa and Warte) of Sargelu Formation are situated in the NE Erbil, the first one Warte is situated near Warte Village (Latitude: 38S 0475516, Longitude: 4041633) and Barzewa near Balak River at Barzewa Village (Latitude: 38S 0467792, Longitude: 4054787), (Fig. 1). Their thicknesses are about 57 m and 56 m for both sections respectively. The lower contact is Sehkanian Formation and the upper contact is Naokelekan Formation for both sections and they are visible outcropped.

During the Jurassic period, the northeastern part of the Arabian plate, including Kurdistan region, was covered by dysoxic to anoxic environmental deposition conditions, which allowed for the preservation of high organic matter and the production of the world's largest oil and gas reserves (Abdula et al., 2015, Al-Ameri and Zumberge, 2012, Beydoun, 1986, Hakimi et al., 2015, Murris, 1980, Pitman et al., 2004). Wetzel (1948) identified and characterized the Sargelu Formation on the Surdash anticline in Iraqi Kurdistan's region, Sulaimani province (Bellen et al., 1959). Various parts of the petroleum system in the Middle East identified by (Murris, 1980), including the Middle Jurassic, in his classic stratigraphic evolution and oil habitat research of the Middle East. Black shales, which are high in organic matter, are critical to the world's natural fuel economy. The majority of shales contain at least 1% organic carbon; a usual range is between 2% and 10% (Tourtelot, 1979). Along with being rich in organic matter, black shales are also rich in metals and sulfides.

In this work ultrasonic wave was used to extract the organic matter. The term "ultrasonic wave" refers to a sound wave with a frequency greater than 20 kHz, which is beyond the range of human hearing. Its frequency can reach up to 100 kHz and a high energy intensity (Mason and Lorimer, 2002). According to (Li et al., 2021) ultrasonic waves are a high-energy mechanical wave capable of generating mechanical vibration, cavitation, and thermal effects (Fig. 2). The industrial application of ultrasonic wave includes a variety of technological processes such as material dispersion under the action of ultrasonic oscillations, creation of stable emulsions (oil or petroleum products in water), extraction, mixing, lixiviation, and sterilization. It is demonstrated that all of these processes can be carried out efficiently only by initiating and maintaining a cavitation process in liquid (in phase of "stable cavitation"). Cavity bubbles generated in a liquid or a liquid dispersed media have the most energy effect on the surrounding liquid during the bubble collapse phase (Abramenko et al., 2008).

The black shale has been investigated in terms of total organic carbon and major, trace and rare earth elements geochemistry. The majority of the oils produced in northern Iraq's Kurdistan Region are believed to have been provided by the Sargelu Formation (Al-Ameri et al., 2014, Hakimi and Najaf, 2016). That paleo-ocean was characterized by mostly dysoxic-anoxic paleoenvironments near the equator and tectonic instability (Sharland et al., 2001), which allowed for the retention of high organic matter and the creation of the world's largest oil and gas

reserves.To better understand the composition of the black shale, the severity of chemical weathering, the paleoclimate, and the formation and maturation of organic matter, this research focuses on mineralogy, inorganic (major oxides, trace and rare-earth elements), and organic geochemistry. The polar organic compounds extraction from the soil samples by ultrasonic irradiation into pure water (as a mobile phase) was studied.

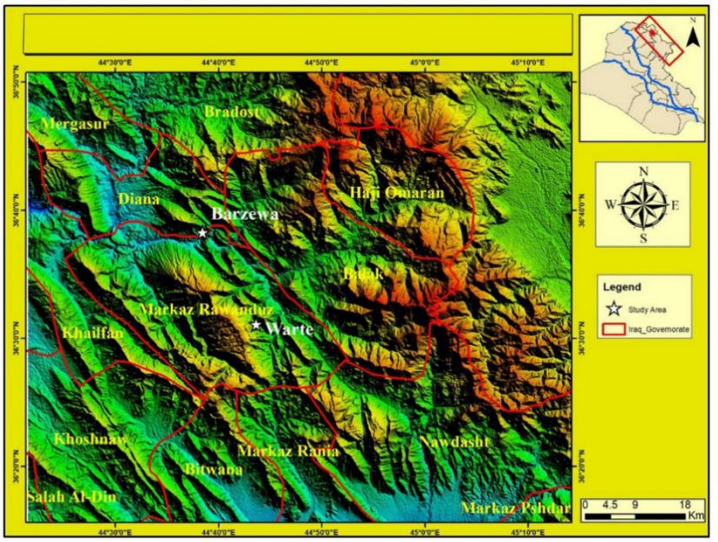

Figure 1. Outcrops of studied Barzewa and Warte locations (Sissakian et al., 2020)

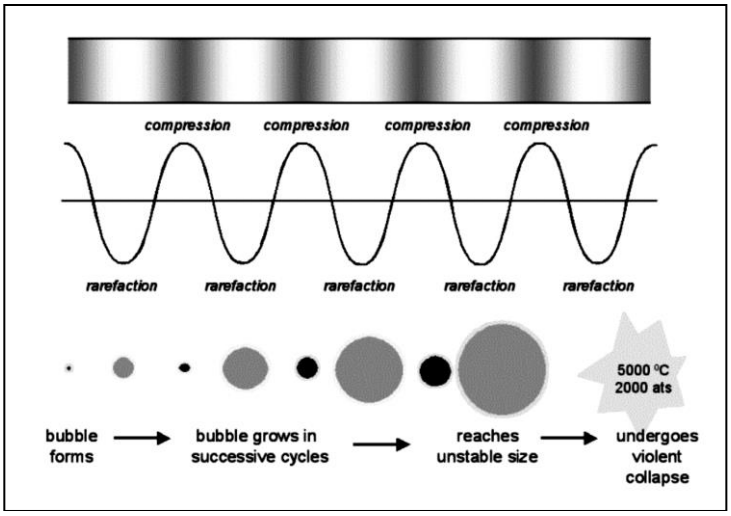

Figure 2. The corresponding relation between microbubble and ultrasonic acting (Mason and Lorimer, 2002)

Geological Setting

The Sargelu Formation is exposed in many locations and outcrops in Iraqi Kurdistan Region (Jassim and Goff, 2006). Across the Paleozoic (570-245 Ma), the Arabian plate was connected to Africa and, along with the nearby blocks consisting of Turkish and Iranian continental portions, formed part of Gondwanaland's long-passive plate border (Beydoun, 1986, Beydoun et al., 1992). Throughout the middle Permian and the Triassic to Jurassic (250 Ma – 160 Ma), extension and rifting separated a succession of microplates from the Arabian portion of Gondwanaland (collectively known as the Cimmerian blocks), which drifted away as the Neo-Tethys Ocean opened, forming the "Arabian Promontory." Additionally, the collision of continental segments of the Eurasian margin with the continental Arabian Plate formed the Zagros Mountain as a result of subduction of the oceanic Arabian Plate crust under the Eurasian Plate and this continent – continent collision started during late Eocene time and the junction continues at present. According to (Martin, 2001), the Middle Jurassic reflects a moment of global sea level rise, and these sediments were deposited in an open-marine environment, since the Arabian Plate (AP) now had passive edges to the northeast and north of Neo-Tethys. The Iraqi Kurdistan including the Sargelu Formation is located in the northern part of the Arabian tectonic Plate.

Materials and Methods

Fieldwork on Sargelu Formation was performed during the autumn of 2021. Two outcrops at (Warte and Barzewa) villages located in the Imbricated Zone in Erbil Governorate were chosen for this study and drawing columnar for both sections (Fig. 3 A&B). Fifteen fresh black shales were collected (seven samples from Warte section and eight samples from Barzewa section). The samples were gathered approximately from the middle part of the Sargelu Formation to the upper contact (Naokelekan Formation). By utilizing X-ray diffraction, the bulk sample powders and clay fractions were analyzed for minerals (XRD). A 30% H2O2 was used to remove the organic materials, which was then washed in distilled water, dried, and mounted on glass slides to produce clay fractions. One untreated slide, one treated with ethylene glycol vapor at 60°C for 1 hour, and three heated for 3 hours at 550°C have been prepared per sample. The Sintag PAD V X-Ray diffractometers with a Ni-filtered Cu-Kα (40 kV and 30 mA) have been used to analyze the bulk samples and the clay fractions. After Li borate fusion, X-ray fluorescence spectrometry (XRF) was used to examine the main oxides (Philips PW-1410 XRF spectrometer, Netherland). ICP-MS has been used to identify trace and rare-earth elements using a four-acid approach that requires HCl, HClO4, HNO3, and HF. Under a perchloric acid fume hood, it takes two days to complete the operation. To calculate the loss on ignition (L.O.I.), sample powders were ignited for six hours at 1000 °C.

Total organic carbon (TOC) and Rock-Eval analyses on fifteen black shale samples were performed at Iran's Research Institute of Petroleum Industry By oxidizing the organic matter in the sample that remains after pyrolysis (in an oxidation furnace set at 600 °C), the Rock Eval II instrument may also be used to estimate the TOC of the sample (residual organic carbon). Remaining organic carbon is measured and added to the organic carbon pyrolyzed by the hydrocarbon

molecules that are released during pyrolysis. The total organic carbon (TOC) is then calculated. Using ultrasound homogenizer (crusher) with power intensity ranged from 100 up to 1800 w and 20Khz frequency, to extract organic compounds from the samples. FTIR (Bruker) alpha II was used for identifying the existence of organic compounds in recovery phase (water).

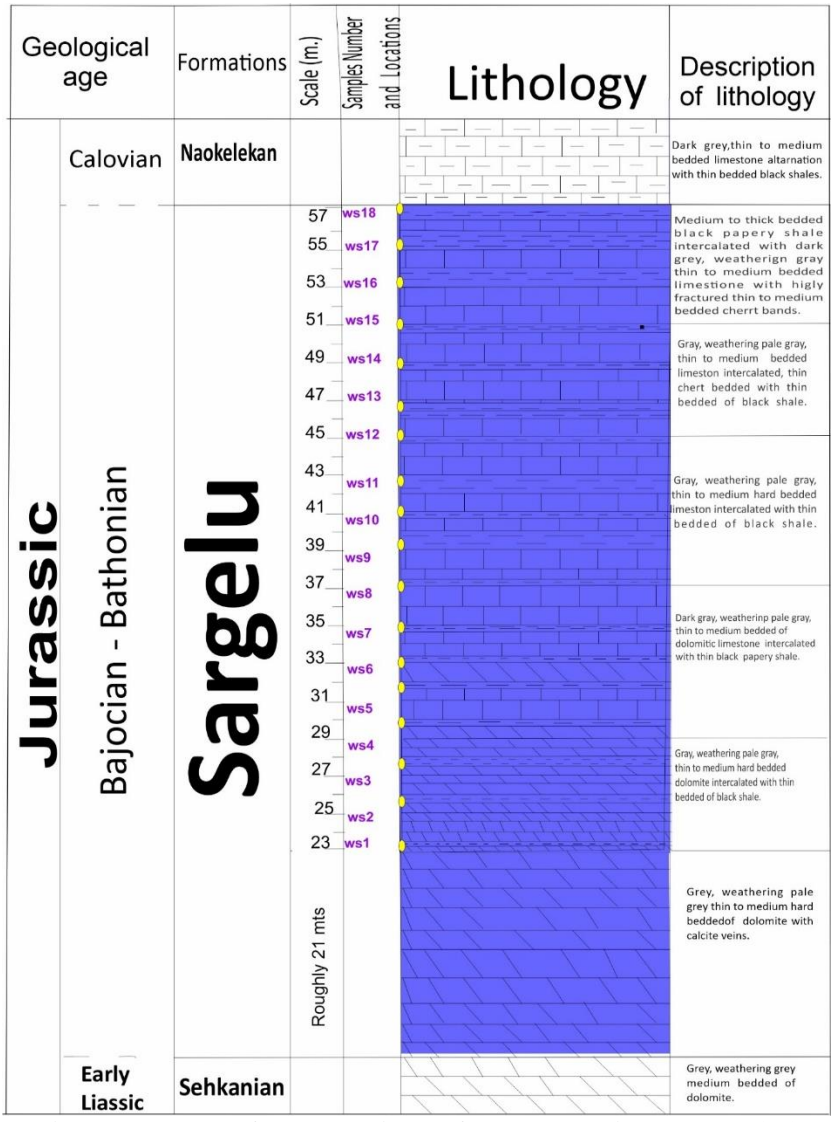

Figure 3A. Sargelu Formation columnar section, Warte (W)

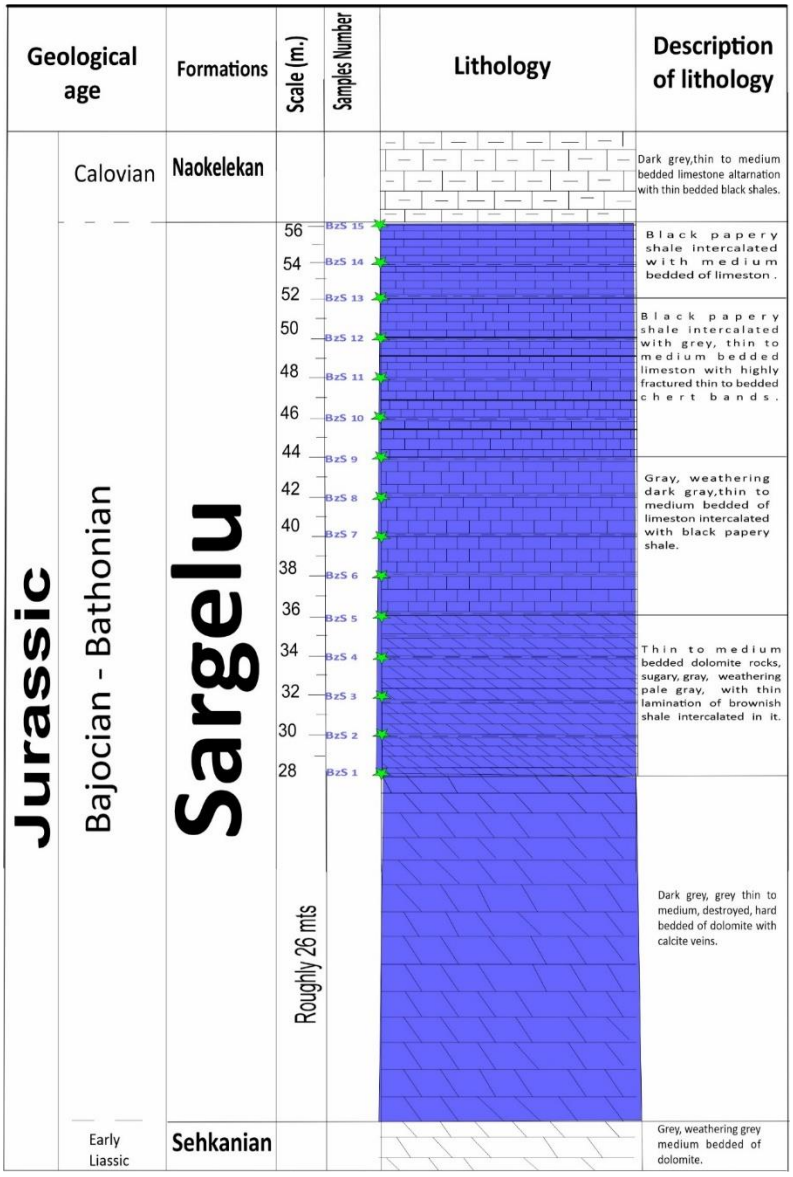

Figure 3B. Sargelu Formation columnar section, Barzewa (Bz)

Results

Mineralogy

Table 1 shows the results of the mineralogical analysis of black shale fractions and bulk samples from the Sargelu formation. In both sections of the black shale, quartz, dolomite, orthoclase, and calcite predominate as non-clay minerals, with minor amounts of gypsum, hematite, pyrite, and albite being found in certain samples. Illite-rich clay fraction. As shown by these results, the clay fractions from the two sites have different mineralogical compositions. (Segonzac, 1970) was estimated the Illite crystallinity index by measuring the width of the 10 A°

peak at half height, the values in the Sargelu black shales range from 0.23 to 0.30° Δ2θ (Table 1). The average IC value in Barzewa is 0.263°Δ2θ, which is slightly lower than the average IC value in Warte, which is 0.266°Δ2θ.

Table 1
Mineralogical composition and illite crystallinity (IC) of black shale, Sargelu Formation.

Sample	Non-clay minerals (wt%)								Caly mineral (wt%)	Illite crystallinity (IC)
	Quartz	Dolomite	Orthoclase	Calcite	Gypsum	Hematite	Pyrite	Albite	Illite	
WS 1	11		3	83						
WS 4	8	55	3	27					4	0.26
WS 6	18	42	4	31					2	0.25
WS 9	10	29	4	53			1			
WS 11	36	6	4	51						
WS 15	22	28	5	35				3	4	0.29
WS 18	5	38	3	49				2		
BS 1	17	25	3	47	1	1			4	0.23
BS 3	19	20	3	52		1			2	0.25
BS 5	20	19	4	47	2	1	1		3	0.24
BS 7	9	21	3	60	2				2	0.25
BS 8	15	19	4	55	1				3	0.27
BS 11	14	16	3	58	2				4	0.29
BS 13	17	31	4	40	2				3	0.30
BS 15	25	14	4	51	1				2	0.28

Geochemistry
Major Oxides

The abundances of major-element chemical data in black shale samples are presented in Table 2. Calcium oxide (CaO) is the dominant constituent with an average of 31.45%, next come SiO2 21.61%, MgO 4.02% and Al2O3 3.74%. The Sargelu black shales have high CaO and MgO because of the prominent of calcite, dolomite, and fossil content. Titanium may be found in clay minerals or the detrital phase, since there are positive relationships between Al2O3 and TiO2. In the Sargelu black shales, there is a positive relationship between K2O, Al2O3, Fe2O3, TiO2, and MnO. This means that potassium is mostly found in the illite part of these rocks. Al2O3 is significant positively correlated with Fe2O3, K2O, and TiO2 (r=0.91, r=0.96, and r=0.99) respectively suggest that they are associated with detrital phases. Also, there is a positive correlation between Fe2O3, MnO, K2O, TiO2, and P2O5. There is a –v correlation between CaO and SiO2, Al2O3, Fe2O3, K2O, and TiO2 due to increasing of carbonate phases at the expense of detrital phases.

Table 2
Major oxides (wt. %), CIA, ICV, SiO_2 (Wt %) of black shale, Sargelu Formaion.

Samples No.	SiO_2	Al_2O_3	Fe_2O_3	CaO	MgO	Na_2O	K_2O	TiO_2	MnO	P_2O_5	LOI	Total	Al_2O_3/SiO_2	Al_2O_3/TiO_2	CIA	ICV	SiO_2 (wt. %)a
WS 1	10.787	1.641	1.362	45.132	1.926	0.01	0.734	0.086	0.012	0.144	38.09	99.92	0.15	19.08	68.81	29.97	62.92
WS 4	13.427	2.617	1.666	32.677	8.804	0	1.027	0.174	0.014	0.133	39.08	99.62	0.19	15.04	71.82	16.88	57.93
WS 6	22.476	3.238	1.305	30.213	7.147	0.032	1.09	0.204	0.015	0.157	33.86	99.74	0.14	15.87	74.27	12.29	58.96
WS 9	13.079	2.021	1.48	40.662	4.086	0.058	0.837	0.133	0.016	0.14	37.43	99.94	0.15	15.20	69.31	23.32	58.12
WS 11	30.403	1.841	1.137	33.162	1.158	0.087	0.649	0.113	0.015	0.202	31.23	99.997	0.06	16.29	71.44	19.67	59.48
WS 15	33.689	4.332	2.034	24.457	2.206	0.161	1.217	0.258	0.011	0.159	31	99.52	0.13	16.79	75.87	6.95	60.09
WS 18	6.45	1.458	1.316	43.541	5.194	0.061	0.594	0.102	0.014	0.148	40.75	99.63	0.23	14.29	69.00	34.79	57.01
BS 1	34.45	13.886	4.249	8.79	4.769	0.106	4.438	0.809	0.028	0.398	25.98	97.90	0.40	17.16	75.34	1.61	60.56
BS 3	28.392	7.235	4.087	15.044	6.664	0.032	3.445	0.445	0.026	0.78	32.43	98.58	0.25	16.26	67.54	4.05	59.44
BS 5	27.028	3.104	2.176	30.891	3.895	0.029	1.353	0.139	0.02	0.596	30.72	99.95	0.11	22.33	69.19	12.36	66.94
BS 7	13.47	2.211	1.539	39.873	2.694	0.053	1.232	0.114	0.012	0.296	38.04	99.53	0.16	19.39	63.24	20.54	63.31
BS 8	19.316	3.88	2.119	32.453	2.223	0.083	1.835	0.222	0.028	0.394	37.35	99.90	0.20	17.48	66.92	9.98	60.94
BS 11	17.457	2.108	1.549	37.128	1.667	0	1.042	0.123	0.01	0.175	38.7	99.96	0.12	17.14	66.92	19.64	60.52
BS 13	21.251	3.575	1.752	30.442	5.432	0.058	1.341	0.184	0.021	0.321	35.06	99.44	0.17	19.43	71.87	10.92	63.35
BS 15	32.542	2.906	1.913	27.213	2.435	0.106	1.258	0.186	0.02	0.275	30.38	99.23	0.09	15.62	68.06	11.34	58.65
Average	21.61	3.74	1.98	31.45	4.02	0.06	1.47	0.22	0.02	0.29	34.67	99.52	0.17	17.16	69.97	15.62	60.55

*a - SiO_2 content calculated based on Al_2O_3/TiO_2 ratio after Hayashi et al. (1997).
CIA = {Al_2O_3 / (Al_2O_3 + CaO* + Na_2O + K_2O)} x 100 (McLennan, 1993, Nesbitt and Young, 1982) ---- after correction
SiO_2 (wt%)= 39.34 + 1.2578 (Al_2O_3/TiO_2) - 0.0109 (Al_2O_3/TiO_2)2

Trace Elements

Table 3 lists the trace element's Data of the black shales from the Sargelu formation. The Upper Continental Crust (UCC) and Post-Archean Australian Shale (PAAS) (Taylor and McLennan, 1985) were used as references to study the differences in trace element content. Vanadium (V) is the highest content in black shale with an average (326.27 ppm) there is a huge different with (UCC) and (PAAS) which are (60.0 ppm and 150.0 ppm) respectively, the next is Zinc (Zn), Nickle (Ni), Cupper (Cu), Uranium (U), and Cromium (Cr) (233.58, 293.71, 71.10, 26.53, 36.95) ppm respectively, the distinctive lower content of trace element from black shale of Sargelu formation is Barium (Ba), Rabidium (Rb), and Zirconium (Zr), (87.69, 22.81, 21.99) ppm respectively compare to (UCC) and (PAAS). The Cobalt (Co) (1.53 ppm), Hafnium (Hf) (0.62 ppm), Thorium (Th) (1.64 ppm), and Yttrium (Y) (20.85 ppm) are slightly lower than the (UCC) and (PAAS). Based on the PAAS normalized diagram the comparison has been made between black shale of the Sargelu Formation and PAAS plus UCC for the trace elements (Fig. 4).

Table 3
Trace Elements (ppm) of black shale, Sargelu Formaion.

Sample/Element	Rb	Sr	Ba	Th	U	Y	Zr	Nb	Hf	Sc	V	Cr	Co	Ni	Cu	Zn	Th/U
WS 1	11.40	342.10	69.40	0.82	21.57	17.7	9.00	0.53	0.28	2.0	189.00	16.00	0.52	182.00	103.70	204.10	0.04
WS 4	25.81	183.70	76.80	1.42	20.65	18.5	18.00	1.79	0.58	3.3	312.00	26.00	1.19	221.00	47.60	225.30	0.07
WS 6	26.52	195.60	77.00	1.76	20.29	14.4	22.00	2.48	0.74	3.8	270.00	24.00	0.25	186.00	61.90	184.40	0.09
WS 9	15.76	338.10	97.20	1.24	19.00	16.0	15.00	1.37	0.49	2.6	230.00	26.00	0.95	167.00	30.50	201.90	0.07
WS 11	15.02	261.50	59.70	1.28	31.45	27.4	17.00	1.15	0.48	3.4	190.00	24.00	0.67	238.00	50.80	174.70	0.04
WS 15	25.75	227.90	95.00	1.93	24.82	30.9	26.00	2.58	0.80	4.9	583.00	41.00	0.53	501.00	61.30	428.20	0.08
WS 18	12.00	254.00	50.40	0.79	19.76	18.9	11.00	1.06	0.34	2.4	405.00	19.00	0.89	132.00	26.30	249.70	0.04
Av. WS	18.89	257.56	75.07	1.32	22.51	20.5	16.86	1.57	0.53	3.2	311.29	25.14	0.71	232.43	54.59	238.33	0.06
BS 1	63.48	205.20	109.80	7.31	34.17	21.1	137.00	13.72	3.62	9.9	625.00	121.00	6.33	463.00	200.80	274.20	0.21
BS 3	31.20	109.50	56.10	1.55	32.33	21.1	17.00	1.06	0.44	3.9	671.00	77.00	4.29	535.00	146.10	312.40	0.05
BS 5	18.25	242.40	71.40	1.44	33.11	22.5	11.00	0.33	0.30	2.9	387.00	44.00	4.04	517.00	90.90	309.60	0.04
BS 7	15.30	260.70	54.30	1.09	22.76	13.2	12.00	0.26	0.27	2.2	128.00	22.00	0.94	243.00	63.00	101.30	0.05
BS 8	20.33	356.50	236.50	1.22	35.45	34.0	10.00	0.17	0.23	3.6	318.00	47.00	0.69	296.00	43.90	434.70	0.03
BS 11	18.51	263.50	122.70	0.60	32.17	15.8	3.00	0.76	0.04	2.1	197.00	25.00	0.31	286.00	43.10	135.90	0.02
BS 13	24.24	227.30	67.50	1.17	27.57	16.5	14.00	0.59	0.38	2.9	210.00	24.00	0.83	219.00	58.50	172.40	0.04
BS 15	22.42	356.30	84.10	1.28	26.80	25.0	13.00	0.23	0.33	3.4	194.00	30.00	1.28	281.00	54.60	90.20	0.05
Av. BZS	26.72	252.68	100.30	1.96	30.55	21.2	27.13	2.14	0.70	3.9	341.25	48.75	2.34	355.00	87.61	228.84	0.06
T. Ave.	22.81	255.12	87.69	1.64	26.53	20.85	21.99	1.85	0.62	3.53	326.27	36.95	1.53	293.71	71.10	233.58	0.06
UCC	112.00	350.00	550.00	10.70	2.80	22.0	190.00	25.00	5.80	11.0	60.00	35.00	10.00	20.00	25.00	71.00	3.82
PAAS	160.00	200.00	650.00	14.60	3.10	27.0	210.00	19.00	5.00	16.0	150.00	110.00	23.00	55.00	50.00	85.00	4.71

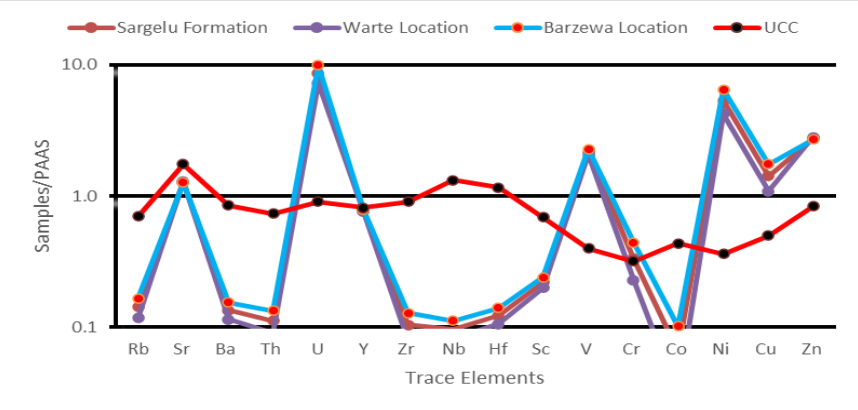

Figure 4. PAAS normalized diagram for trace elements of the black shale of Sargelu Formation (PAAS values after Taylor and McLennan, 1985)

Rare Earth Elements

Table 4 lists the rare-earth element (REE) content of the black shales from the Sargelu formation. The sum of rare-earth elements (Σ REE) varies from 45.81 to 143.12 ppm with an average (69.42 ppm). REE in the examined black shales are normalized to levels for the (PAAS) as reported by Taylor and McLennan (1985). Based on the chondrite normalized pattern the comparison has been made between black shale of the Sargelu Formation and PAAS plus UCC for the trace elements (Fig. 5). The chondrite normalized pattern of rare-earth elements in this study appears with an enrichment of LREEs and the similar trends of the black shale for the two sections indicate that they are from the same origin. While the HREEs relatively with flat pattern, and the samples mostly have the negative Eu.

Table 4
Rare Earth Elements (ppm) of black shale, Sargelu Formation.

Sample/Element	La	Ce	Pr	Nd	Sm	Eu	Gd	Tb	Dy	Ho	Er	Tm	Yb	Lu	Σ REE
WS 1	14.3	20.0	2.6	9.3	2.0	0.5	1.8	0.4	1.6	0.4	1.1	0.2	0.9	0.1	55.09
WS 4	16.4	24.2	2.8	10.4	2.4	0.6	2.0	0.5	1.9	0.4	1.4	0.2	1.1	0.2	64.66
WS 6	12.3	21.8	2.4	8.8	2.0	0.5	1.7	0.4	1.5	0.4	1.1	0.2	1.0	0.1	54.27
WS 9	12.8	17.6	2.3	8.4	1.9	0.6	1.6	0.4	1.5	0.4	1.1	0.2	0.8	0.1	49.51
WS 11	15.1	21.5	3.5	13.4	3.0	0.8	2.7	0.6	2.5	0.6	1.8	0.3	1.4	0.2	67.36
WS 15	21.5	38.8	4.2	16.7	3.8	1.0	3.4	0.8	3.1	0.7	2.3	0.4	1.9	0.3	98.82
WS 18	15.1	24.0	2.0	7.5	1.7	0.6	1.6	0.5	1.4	0.4	1.3	0.3	1.3	0.2	57.65
Ave. WS	15.3	24.0	2.8	10.6	2.4	0.7	2.1	0.5	1.9	0.5	1.4	0.2	1.2	0.2	63.91
BS 1	26.2	74.3	5.3	20.6	4.6	1.0	3.3	0.7	2.7	0.6	1.8	0.3	1.5	0.3	143.12
BS 3	14.3	39.9	2.5	10.3	2.3	0.6	2.1	0.5	1.9	0.4	1.4	0.2	1.1	0.2	77.47
BS 5	18.6	30.9	3.3	13.0	2.9	0.7	2.6	0.6	2.0	0.5	1.4	0.2	1.1	0.2	77.86
BS 7	12.6	14.8	2.6	8.4	1.8	0.5	1.5	0.3	1.2	0.3	0.8	0.1	0.6	0.1	45.81
BS 8	16.0	23.1	4.2	17.2	4.0	1.1	3.3	0.8	2.9	0.7	2.1	0.3	1.6	0.3	77.31
BS 11	13.2	22.5	2.3	9.0	1.9	0.6	1.6	0.4	1.4	0.4	1.1	0.2	0.9	0.1	55.45
BS 13	14.2	22.7	2.8	10.2	2.3	0.6	1.9	0.5	1.7	0.4	1.2	0.2	0.9	0.2	59.61
BS 15	14.6	18.4	3.6	13.4	3.0	0.8	2.5	0.6	2.3	0.5	1.6	0.2	1.3	0.2	62.84
Ave. BZS	16.2	30.8	3.3	12.8	2.9	0.7	2.3	0.5	2.0	0.5	1.4	0.2	1.1	0.2	74.93
T. Ave.	15.8	27.4	3.1	11.7	2.6	0.7	2.2	0.5	2.0	0.5	1.4	0.2	1.2	0.2	69.42
UCC	30.0	64.0	7.1	26.0	4.5	0.9	3.8	0.6	3.5	0.8	2.3	0.3	2.2	0.3	146.37
PAAS	38.2	79.6	8.8	33.9	5.6	1.1	4.7	0.8	4.7	1.0	2.9	0.4	2.8	0.4	184.76

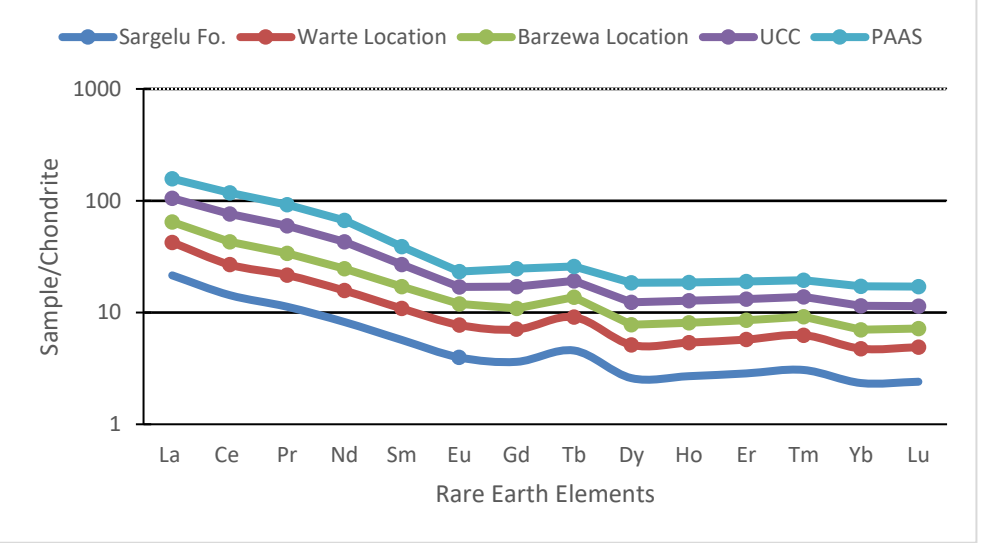

Figure 5. Chondrite normalized rare earth elements of the black shale of Sargelu Formation (Chondrite normalized values are from Taylor and McLennan, 1985).

Organic geochemistry

The fifteen samples of black shale from the Sargelu formation were analyzed using total organic carbon (TOC) content and Rock-Eval analysis, as well as the results are reported in Table 5. TOC contents values 2.0 – 4.0 wt% indicate very good source rooks, whereas those above 4.0 wt.% point to excellent source rook (Peters and Cassa, 1994). In the Sargelu black shale, TOC content ranges from 0.95% to 13.88 wt%, with an average of 4.29 wt%. In the Sargelu Formation's black shales, the quantity of hydrocarbons (S2) released during pyrolysis ranges from 0.03 to 7.85, with an average of 2.12. Depending on (TOC versus S2) plotting after (Langford and Blanc-Valleron, 1990) the analyzed black shale contains kerogen Type II - III which is imply the terrestrial origin (Fig. 6).

Table 5
Total organic carbon (TOC) contents and Rock-Eval analysis (hydrocarbon quality S2) of black shale, Sargelu Formation.

Sample	TOC	S2
WS 1	1.62	0.23
WS 4	1.4	0.13
WS 6	0.95	0.1
WS 9	2.2	0.29
WS 11	0.95	0.03
WS 15	2.62	0.1
WS 18	1.12	0.07
BS 1	6.93	2.59
BS 3	13.88	7.85
BS 5	7.28	4.75

BS 7	4.1	2.99
BS 8	3.52	0.55
BS 11	7.64	6.62
BS 13	3.88	2.55
BS 15	6.23	2.98
Average	4.29	2.12

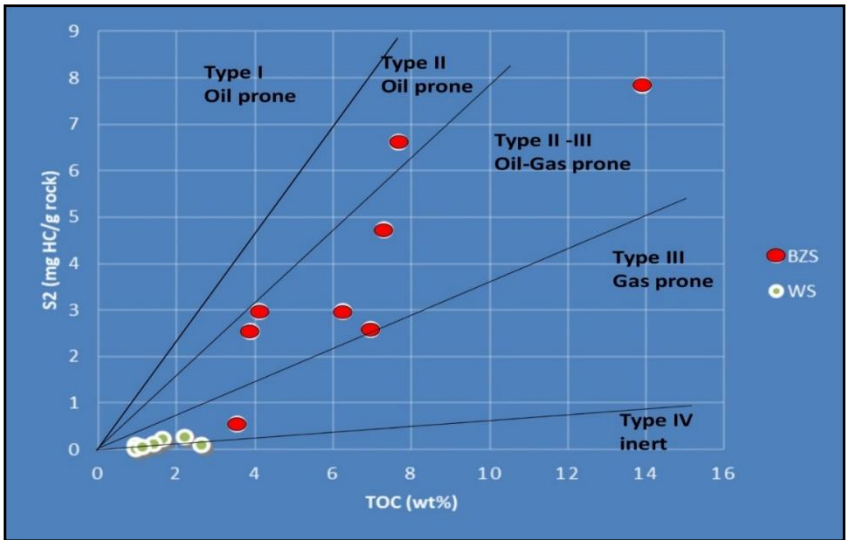

Figure 6. Plot of S2 versus TOC (Langford and Blanc-Valleron, 1990)

Ultrasonic irradiation chemical effect

Three types of samples (sample one, two, and three) were depended in this work. These samples were mixed with water (as mobile phase). Ultrasonic device (Toption Group, TU-1800E) was used with different power intensity (watts) to crash the structure of solid molecules. This action helped to recover the polar organic compounds into water. The details of ultrasound processes on three black shale samples at different power intensities (watts), and times of processing are shown in table (6). The chemical effect result of ultrasound homogenizer processing were analyzed by using infrared spectroscopy device (FTIR-Bruker-alpha II) which is the one of the most common applications for identification of polar organic compounds. FTIR analyzing showed existence of hydrocarbon compounds contain C-H and C-C bonds in recovery phase (pure water). Figure (7) shows that hydrocarbon compound was recover which its peak was about 1392 cm^{-1} (C-H) band area.

Table 6 Black Shale Tested by Ultrasound Homogenizer							
Sample 1 (BS12)	Frequency	Time	Weight	Beaker's Volume	Water Filling	Pulse	Temperature
Test 1	10% (180Wt)	10 mints	20 gr	250 Ml	125 Ml	2/Sec	27 C
Test 2	40% (720 Wt)	10 mints	20 gr	250 Ml	125 Ml	2/Sec	60 C
Test 3	80% (1440 Wt)	10 mints	20 gr	250 Ml	125 Ml	2/Sec	70 C
Test 4	80% (1440 Wt)	20 mints	20 gr	250 Ml	125 Ml	2/Sec	77 C
Sample 2 (BS2)/ Test1	40% (720 Wt)	20 mints	25 gr	500 Ml	250 Ml	2/Sec	49 C
Test 2	60% (1080 Wt)	20 mints	25 gr	500 Ml	250 Ml	2/Sec	59 C
Test 3	70% (1260 Wt)	20 mints	25 gr	500 Ml	250 Ml	2/Sec	60 C
Test 4	80% (1440 Wt)	20 mints	25 gr	500 Ml	250 Ml	2/Sec	64 C
Test 5	80% (1440 Wt)	30 mints	25 gr	500 Ml	250 Ml	2/Sec	72 C
Sample 3 (WS9)/ Test1	70% (1260 Wt)	30 mints	25 gr	500 Ml	250 Ml	2/Sec	76 C
Test 2	80% (1440 Wt)	30 mints	25 gr	500 Ml	250 Ml	2/Sec	75 C
Test 3	90% (1620 Wt)	30 mints	25 gr	500 Ml	250 Ml	2/Sec	77 C
Test 4	100% (1800 Wt)	30 mints	25 gr	500 Ml	250 Ml	2/Sec	79 C

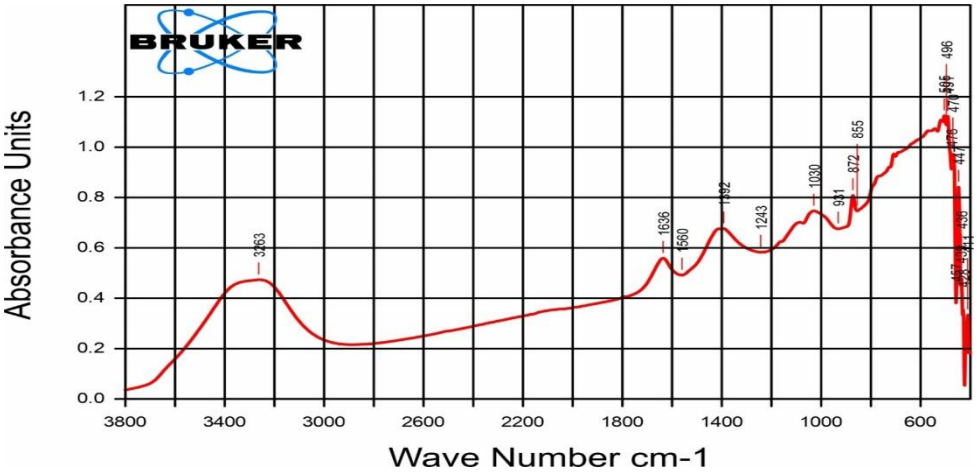

Figure 7. FTIR (Fourier Transform Infrared Spectroscopy) spectrum

Discussions

Weathering intensity and composition of source area

Attempts to investigate their source composition and to hypothesize about the paleoclimate conditions that existed at the time of their formation. Because both Al and Ti are basically immobile in aquatic conditions and there is only a small fractionation of this ratio throughout sediment transport of Ti-and Al-bearing detrital materials, the Al2O3/TiO2 ratio is used as a main indication of the composition of the source rock (Yamamoto et al., 1986). In most igneous rocks, the alumina and titanium content are largely controlled by feldspars and mafic minerals (such as biotite, pyroxene, hornblende, magnetite, and ilmenite), as shown by the gradual rise in the Al/Ti ratio with increasing SiO2 values. This is also reflected in the fact that the Al/Ti ratio gradually increases with increasing SiO2 values (Moosavirad et al., 2011). The Al2O3/TiO2 ratio of mafic igneous

rocks (52 wt% SiO2) is 3–8, that of intermediate igneous rocks (53–66 wt% SiO2) is 8–21, and that of felsic igneous rocks (66–76 wt% SiO2) is 21–70 (Dai et al., 2015, He et al., 2011). A sample of black shales from the Sargelu Formation has an Al2O3/TiO2 ratio of 22.33, which indicates that their parent rocks are intermediate in composition (Table 2). It is possible to utilize the Al2O3/TiO2 ratio of the siliciclastic sediments formed from an igneous source rock in order to determine the SiO2 content of the sediments (Hayashi et al., 1997):

$$SiO2\ (wt.\ \%) = 39.34 + 1.2578(Al2O3/TiO2)\ 0.0109(Al2O3/TiO2)2$$

The calculated values are listed in (Table 2) and range from 57.01 to 66.94 with an average (60.55 w%) for the Sargelu black shales that is indicating an intermediate nature of the source rocks. For the easiest way to determine whether or not sediments have been recycled, calculate the sediment's compositional maturity. Cox et al. (1995) suggested the Index of Compositional Variability (ICV) may be used to measure the compositional maturity index. The following equation is used to compute ICV values: (Cox et al., 1995):

$$ICV = (Fe2O3 + K2O + Na2O + CaO + MgO + MnO)/Al2O3$$

The ICV values in the black shales from the Sergalu formation ranging from 1.61 to 34.79. Feldspars, amphiboles, and pyroxenes would all have a value greater than 1 (Table 2). Using the Al2O3/SiO2 ratio, a sediment source terrain's chemical weathering intensity may also be determined (Dai et al., 2012). This ratio grows as weathering progresses, and so represents the paleo-climate conditions. An intermediate chemical weathering process is suggested by similar Chemical Index of Alteration (CIA) values seen in black shale (McLennan, 1993, Nesbitt and Young, 1982) (Table 2). Th/U ratios may rise as a consequence of chemical weathering, as sedimentary rocks lose U as a result of oxidation (McLennan et al., 1995, McLennan and Taylor, 1991). The CIA evidence on intermediate weathering is supported by Th/U ratios in the investigated shales, which vary from 0.02 to 0.21. The Th is lower in the black shales than in the rest of the upper continental crust, but the U is greater, indicating a felsic source (Rudnick et al., 2003) (Table 3).

Maturation and source of organic matter

Phyllosilicates' diagenetic/metamorphic recrystallization is often measured using the illite crystallinity index (IC). Thermal overprinting increases the crystallinity of illite, which lowers the IC value. So the diagenetic/low-grade metamorphic zone was divided using the IC index and the change of smectite to illite (Frey and Seilacher, 1980, Rainer et al., 2002). The IC > 0.42° 2 is a late-stage diagnostic illite, whereas the anchizone is defined by values between 0.42 and 0.25° 2, and the epizone by values IC 0.25 A°20 (Kübler and Jaboyedoff, 2000). The IC value is 0.23 – 0.30° Δ2θ of the black shales from the Sargelu formation indicate the high anchizone exception two samples are in the epizone stage. Table 1 shows that the illite concentration is just 2–4%, which is lower than what would be anticipated in rocks that are over-mature. (Dellisanti et al., 2010). By looking at their hydrocarbon yields (S2), the kerogen type can be evaluated (Espitalié and Bordenave, 1993, Peters and Cassa, 1994). There are Type II and Type III

kerogens in the examined black shales, as shown by the S2 vs TOC plot (Fig. 7) (Langford and Blanc-Valleron, 1990). Organic matter found in the black shales studied is likely to have come from a terrestrial origin based on the amount of Type III kerogen.

Hydrocarbons analysis

With using the ultrasound homogenizer, we got the C-H bond which is transfer from the sold state to the liquid state without adding any chemical ingredients. Experimentally at low power intensity(watts), and time less than 30 minutes no result was obtained from ultrasonic processing. The hydrocarbon components were recovered from the sold black shale sample by gradual increasing of power intensity for time intervals more than 30 minutes. It means that the higher ultrasound power, better recovery of the organic compounds.

Conclusion

Using inorganic geochemistry (major oxides, trace and rare-earth elements), mineralogy, and organic geochemistry for the Sargelu Formation's black shale, we were able to determine the composition of the source area as well as the origin and maturation of organic matter. Moreover, recover the polar organic compounds from the soil samples into water. The Sargelu Black Shale Formation's Al2O3/TiO2, Rb/Sr ratios, and SiO2 composition indicate that the source rocks were intermediate to felsic in character. According to the Chemical Index of Alteration (CIA) values in black shale, this intermediate chemical weathering is indicative of the paleoclimate conditions. The IC values and illite contents shows as that the Sargelu Formation in both locations are in the high anchizone stage. The studied black shale contains Type II - III kerogen which is imply the terrestrial origin. By gradual increasing of power intensity the hydrocarbon components were recovered from the solid black shale.

References

ABDULA, R. A., BALAKY, S. M., NURMOHAMADI, M. & PIROUI, M. 2015. Microfacies analysis and depositional environment of the Sargelu Formation (Middle Jurassic) from Kurdistan Region, northern Iraq. Donnish Journal of Geology and Mining Research, 1, 001-026.

ABRAMENKO, D. S., LEVIN, S. N., KHMELEV, S. S. & KUZOVNIKOV, Y. M. The ultrasonic flowing reactor for intensive ultrasonic processing of liquids in thin layer. 2008 9th International Workshop and Tutorials on Electron Devices and Materials, 2008. IEEE, 219-222.

AL-AMERI, T. K. & AL-NAGSHBANDI, S. F. 2015. Age assessments and palynofacies of the Jurassic oil source rocks succession of North Iraq. Arabian Journal of Geosciences, 8, 759-771.

AL-AMERI, T. K. & ZUMBERGE, J. 2012. Middle and upper jurassic hydrocarbon potential of the zagross fold Belt, North Iraq. Marine and Petroleum Geology, 36, 13-34.

AL-AMERI, T. K., NAJAF, A. A., AL-KHAFAJI, A. S., ZUMBERGE, J. & PITMAN, J. 2014. Hydrocarbon potential of the Sargelu formation, North Iraq. Arabian Journal of Geosciences, 7, 987-1000.

AQRAWI, A., GOFF, J., HORBURY, A. & SADOONI, F. 2010. The petroleum Geology of Iraq. Scientific press Ltd. Beaconsfield UK.
BELLEN, R. V., DUNNINGTON, H., WETZEL, R. & MORTON, D. 1959. Lexique stratigraphique international. Asie, Iraq, 3, 324.
BEYDOUN, Z. 1986. The petroleum resources of the Middle East: a review. Journal of Petroleum Geology, 9, 5-27.
BEYDOUN, Z., CLARKE, M. H. & STONELEY, R. 1992. Petroleum in the Zagros basin: a late tertiary foreland basin overprinted onto the outer edge of a vast hydrocarbon-rich paleozoic-mesozoic passive-margin shelf: chapter 11.
BUDAY, T. 1980. The regional geology of Iraq: stratigraphy and paleogeography, State Organization for Minerals, Directorate General for Geological Survey ….
COX, R., LOWE, D. R. & CULLERS, R. 1995. The influence of sediment recycling and basement composition on evolution of mudrock chemistry in the southwestern United States. Geochimica et Cosmochimica Acta, 59, 2919-2940.
DAI, L. Q., ZHAO, Z. F., ZHENG, Y. F. & ZHANG, J. 2015. Source and magma mixing processes in continental subduction factory: Geochemical evidence from postcollisional mafic igneous rocks in the D abie orogen. Geochemistry, Geophysics, Geosystems, 16, 659-680.
DAI, S., REN, D., CHOU, C.-L., FINKELMAN, R. B., SEREDIN, V. V. & ZHOU, Y. 2012. Geochemistry of trace elements in Chinese coals: a review of abundances, genetic types, impacts on human health, and industrial utilization. International Journal of Coal Geology, 94, 3-21.
DELLISANTI, F., PINI, G. A. & BAUDIN, F. 2010. Use of Tmax as a thermal maturity indicator in orogenic successions and comparison with clay mineral evolution. Clay minerals, 45, 115-130.
ESPITALIÉ, J. & BORDENAVE, M. 1993. Screening techniques for source rocks evaluation; tools for source rocks routine analysis; Rock-Eval pyrolysis. Applied petroleum geochemistry: Paris, Editions Technip, 261-273.
FREY, R. W. & SEILACHER, A. 1980. Uniformity in marine invertebrate ichnology. Lethaia, 13, 183-207.
HAKIMI, M. H. & NAJAF, A. A. 2016. Origin of crude oils from oilfields in the Zagros Fold Belt, southern Iraq: Relation to organic matter input and paleoenvironmental conditions. Marine and Petroleum Geology, 78, 547-561.
HAKIMI, M. H., MOHIALDEEN, I. M., ABDULLAH, W. H., WIMBLEDON, W., MAKEEN, Y. M. & MUSTAPHA, K. A. 2015. Biomarkers and inorganic geochemical elements of Late Jurassic-Early Cretaceous limestone sediments from Banik Village in the Kurdistan Region, Northern Iraq: implications for origin of organic matter and depositional environment conditions. Arabian Journal of Geosciences, 8, 9407-9421.
HAYASHI, K.-I., FUJISAWA, H., HOLLAND, H. D. & OHMOTO, H. 1997. Geochemistry of~ 1.9 Ga sedimentary rocks from northeastern Labrador, Canada. Geochimica et cosmochimica acta, 61, 4115-4137.
HE, J., DUAN, Y., ZHANG, X., WU, B. & XU, L. 2011. Hydrocarbon generation conditions of the shale in niutitang formation of lower cambrian, southern chongqing and northern Guizhou. Marine Geology Frontiers, 27, 34-40.
JASSIM, S. Z. & GOFF, J. C. 2006. Geology of Iraq, DOLIN, sro, distributed by Geological Society of London.
KÜBLER, B. & JABOYEDOFF, M. 2000. Illite crystallinity. Comptes Rendus de l'Académie des Sciences-Series IIA-Earth and Planetary Science, 331, 75-89.

LANGFORD, F. & BLANC-VALLERON, M.-M. 1990. Interpreting Rock-Eval pyrolysis data using graphs of pyrolizable hydrocarbons vs. total organic carbon. AAPG bulletin, 74, 799-804.

LI, X., ZHANG, J., WU, C., HONG, T., ZHENG, Y., LI, C., LI, B., LI, R., WANG, Y. & LIU, X. 2021. Experimental Research on the Effect of Ultrasonic Waves on the Adsorption, Desorption, and Seepage Characteristics of Shale Gas. ACS omega, 6, 17002-17018.

MARTIN, A. Z. 2001. Late Permian to Holocene paleofacies evolution of the Arabian Plate and its hydrocarbon occurrences. GeoArabia, 6, 445-504.

MASON, T. J. & LORIMER, J. P. 2002. Applied sonochemistry: the uses of power ultrasound in chemistry and processing, Wiley-Vch Weinheim.

MCLENNAN, S. & TAYLOR, S. 1991. Sedimentary rocks and crustal evolution: tectonic setting and secular trends. The Journal of geology, 99, 1-21.

MCLENNAN, S. M. 1993. Weathering and global denudation. The Journal of Geology, 101, 295-303.

MCLENNAN, S., HEMMING, S., TAYLOR, S. & ERIKSSON, K. 1995. Early Proterozoic crustal evolution: Geochemical and NdPb isotopic evidence from metasedimentary rocks, southwestern North America. Geochimica et Cosmochimica Acta, 59, 1153-1177.

MOOSAVIRAD, S., JANARDHANA, M., SETHUMADHAV, M., MOGHADAM, M. & SHANKARA, M. 2011. Geochemistry of lower Jurassic shales of the Shemshak Formation, Kerman Province, Central Iran: Provenance, source weathering and tectonic setting. Geochemistry, 71, 279-288.

MURRIS, R. 1980. Middle East: stratigraphic evolution and oil habitat. AAPG Bulletin, 64, 597-618.

NESBITT, H. & YOUNG, G. 1982. Early Proterozoic climates and plate motions inferred from major element chemistry of lutites. nature, 299, 715-717.

PETERS, K. E. & CASSA, M. R. 1994. Applied source rock geochemistry: Chapter 5: Part II. Essential elements.

PITMAN, J. K., STEINSHOUER, D. & LEWAN, M. D. 2004. Petroleum generation and migration in the Mesopotamian Basin and Zagros Fold Belt of Iraq: results from a basin-modeling study. GeoArabia, 9, 41-72.

RAINER, T., HERLEC, U., RANTITSCH, G., SACHSENHOFER, R. F. & VRABEC, M. 2002. Organic matter maturation vs clay mineralogy: A comparison for Carboniferous to Eocene sediments from the Alpine-Dinaride junction (Slovenia, Austria). Geologija, 45, 513-518.

RUDNICK, R., GAO, S., HOLLAND, H. & TUREKIAN, K. 2003. Composition of the continental crust. The crust, 3, 1-64.

SEGONZAC, G. D. 1970. Transformation of clay minerals during diagenesis and low-grade metamorphism: a review. Sedimentology.

SHARLAND, P., CASEY, D., DAVIES, R., SIMMONS, M. & SUTCLIFFE, O. 2001. Arabian plate sequence stratigraphy (Vol. 2, p. 371). Bahrain: Gulf PetroLink.

SISSAKIAN, V. K., AL-ANSARI, N. & ABDULLAH, L. H. 2020. Neotectonic activity using geomorphological features in the Iraqi Kurdistan region. Geotechnical and Geological Engineering, 38, 4889-4904.

Suryasa, I. W., Rodríguez-Gámez, M., & Koldoris, T. (2021). Get vaccinated when it is your turn and follow the local guidelines. *International Journal of Health Sciences*, *5*(3), x-xv. https://doi.org/10.53730/ijhs.v5n3.2938

TAYLOR, S. R. & MCLENNAN, S. M. 1985. The continental crust: its composition and evolution.

TOURTELOT, H. A. 1979. Black shale—its deposition and diagenesis. Clays and clay minerals, 27, 313-321.

YAMAMOTO, K., SUGISAKI, R. & ARAI, F. 1986. Chemical aspects of alteration of acidic tuffs and their application to siliceous deposits. Chemical Geology, 55, 61-76.